0026-895X/05/6805-1291–1300$20.00
MOLECULAR PHARMACOLOGY
Copyright © 2005 The American Society for Pharmacology and Experimental Therapeutics
Mol Pharmacol 68:1291–1300, 2005

Vol. 68, No. 5
15982/3060233
Printed in U.S.A.

Comparative Models of $GABA_A$ Receptor Extracellular and Transmembrane Domains: Important Insights in Pharmacology and Function[S]

Margot Ernst, Stefan Bruckner, Stefan Boresch, and Werner Sieghart

Center for Brain Research, Division of Biochemistry and Molecular Biology, Medical University of Vienna, Vienna, Austria (M.E., S.Br., W.S.); and Department of Biomolecular and Structural Chemistry, University of Vienna, Vienna, Austria (S.Bo.)

Received June 26, 2005; accepted August 15, 2005

ABSTRACT

Comparative models of the extracellular and transmembrane domains of $GABA_A$ receptors in the agonist-free state were generated based on the recently published structures of the nicotinic acetylcholine receptor. The models were validated by computational methods, and their reliability was estimated by analyzing conserved and variable elements of the cys-loop receptor topology. In addition, the methodological limits in the interpretation of such anion channel receptor models are discussed. Alignment ambiguities in the helical domain were resolved for helix 3 by placing two gaps into the linker connecting helices 2 and 3. The resulting models were shown to be consistent with a wide range of pharmacological and mutagenesis data from $GABA_A$ and glycine receptors. The loose packing of the models results in a large amount of solvent-accessible space and offers a natural explanation for the rich pharmacology and the great flexibility of these receptors that are known to exist in numerous drug-induced conformational states. Putative drug binding pockets found within and between subunits are described, and amino acid residues important for the action and subtype selectivity of volatile and intravenous anesthetics, barbiturates, and furosemide are shown to be part of these pockets. The entire helical domain, however, seems to be crucial not only for binding of drugs but also for transduction of binding to gating or of allosteric modulation. These models can now be used to design new experiments for clarification of pharmacological and structural questions as well as for investigating and visualizing drug induced conformational changes.

$GABA_A$ receptors mediate a large part of the fast inhibitory transmission in the central nervous system and are the targets for many clinically important drugs, such as sedatives, hypnotics, anxiolytics, anticonvulsives, muscle relaxants, and anesthetics (Sieghart, 1995). They are composed of five subunits that can belong to different homologous subunit classes and form a chloride channel that can be opened by GABA. Individual neurons can express many different subunits, resulting in the formation of a large variety of functionally different receptor subtypes (Sieghart and Sperk, 2002). Depending on the subunit composition, these receptors exhibit a distinct pharmacology (Sieghart, 1995).

The subunit organization with the extracellular ligand binding domain containing the "signature" disulfide, four transmembrane segments, and a large variable cytoplasmic domain (termed the "cytoplasmic loop") of unknown structure, as well as the receptor organization as a pentamer, are hallmarks of the superfamily of cys-loop receptors (pentameric ligand-gated ion channels) comprising the cation-conducting nicotinic acetylcholine (nACh) and serotonin type 3 ($5HT_3$-) receptors and the anion-conducting $GABA_A$ and glycine receptors.

In 2001, the X-ray crystallographic structure of acetylcholine binding protein (AChBP) has revealed the fold in which the β-strand rich "extracellular domain" of the superfamily is organized (Brejc et al., 2001). Since then, comparative models of the extracellular domain of different receptors based on this structure have been generated (for review, see Ernst et al., 2003).

After the release of the AChBP structure, cryo-EM images of ACh free and bound preparations of electric fish organ nicotinic receptors have been analyzed by fitting the core of the AChBP X-ray structure into the two sets of EM density maps (Unwin et al., 2002). The ACh bound state turned out to be pseudosymmetrical, with all subunits in the conformation that corresponds with the HEPES bound conformation of AChBP subunits. The ACh free (tense) state, on the other

This work was supported by grant P16397 of the Austrian Science Fund.
[S] The online version of this article (available at http://molpharm.aspetjournals.org) contains supplemental material.
Article, publication date, and citation information can be found at http://molpharm.aspetjournals.org.
doi:10.1124/mol.105.015982.

ABBREVIATIONS: nACh, nicotinic acetylcholine; AChBP, acetylcholine binding protein; EM, electron microscopy; PDB, Protein Data Bank.

hand, was found to be conformationally asymmetrical. The extracellular domain of the two α subunits (that form the plus-sides of the ACh pockets) is in a conformation distinct from the β, γ, and δ subunits' extracellular domain (Unwin et al., 2002).

The structure of the ion pore domain fragment of the torpedo nACh receptor was published in 2003 (Miyazawa et al., 2003) as a 4-Å model in the resting state [Protein Data Bank (PDB) identifier 1OED]. It also has been derived from cryo-EM images, and confirmed the notion that the transmembrane domain of cys-loop receptors is organized as a 4-helix bundle (Bertaccini and Trudell, 2001). Shortly thereafter, a first model combining the extracellular and transmembrane domains of the nicotinic receptor has been discussed (Unwin, 2003) that was eventually published in a refined version (Unwin, 2005) and released with the PDB identifier 2BG9.

This work is the first attempt to integrate all published structural information from the nACh receptor in the closed state into comparative models of $GABA_A$ receptors, with special emphasis on the helical domain. These models were then validated by computational tools as well as by comparison with experimental results. Finally, they were used to explain and consolidate experimental data.

Materials and Methods

Nomenclature Conventions. Amino acid sequence numbering corresponds to the mature protein. In the helix 2 segment, the primed index-numbering scheme is used as well. Whenever individual amino acid residues are named in the text, their residue number in mature rat protein ($GABA_A$ receptors) or torpedo fish (nACh receptor) is indicated, the corresponding position in homologs is often provided in parenthesis as reading aid. Domains of cys-loop receptors have traditionally been termed "extracellular ligand binding domain", "transmembrane domain", and "cytoplasmic loop". Because it is known that the so-called extracellular ligand binding domain and the so-called transmembrane domain form independent folding units that are of predominantly β-stranded and helical character, respectively, we will refer to them as "β-folded domain" and "helical domain". This is particularly appropriate as the helical folding unit is only partially inserted into the membrane and extends significantly (~10 Å) beyond the lipid bilayer into the extracellular compartment (Miyazawa et al., 2003). Few structural data are available on the cytoplasmic "loop", but there is evidence for significant helix contents (Peters et al., 2004; Unwin, 2005). We refer to this putative independent folding unit as "cytoplasmic domain".

Modeling. Standard modeling techniques were used to perform the individual modeling steps. The structure files 1I9B (Brejc et al., 2001), 1OED (Miyazawa et al., 2003), and 2BG9 (Unwin, 2005) were obtained from the PDB. Subunit correspondence between the nACh receptor structures and $GABA_A$ receptors was assigned based on functional homology. Thus, the nACh receptor α subunits, which form the principal side of the ACh binding pocket, and the $GABA_A$ receptor β subunits, which form the principal side of the GABA pocket, correspond to each other, as indicated in Fig. 1b.

All other subunit correspondences follow then inevitably from the respective receptor subunit arrangements. The nACh and $GABA_A$ receptor subunit sequences were then aligned with the appropriate 1OED, 2BG9, and 1I9B subunits with FUGUE (Shi et al., 2001). The resulting sequence-to-structure alignment problems have been discussed extensively for the β-folded domain (Ernst et al., 2003). Here, we focus on the helical domain, where the sequence identity shared between $GABA_A$ receptor subunits and the corresponding 1OED/2BG9 segments ranges from 13 to 21%. Additional alignments were scored and investigated with ClustalX (Thompson et al., 1994). A representative multi sequence alignment and some possible alignment variants are provided in Fig. 1, a and c, and will be discussed below in the section on variable regions.

Coordinate manipulations needed for rotation of the individual sheets of the nACh receptor α subunit (Unwin et al., 2002) and for docking 1OED with nACh receptor extracellular domain models were performed with the Molecular Modeling Tool Kit MMTK (Hinsen, 2000). Comparative modeling, model scoring, and selection were performed as described previously (Ernst et al., 2003), using Modeler version 6 (Sali and Blundell, 1993; Marti-Renom et al., 2000). The $GABA_A$ receptor subtype $\alpha_1\beta_2\gamma_2$ was investigated most extensively; other subtypes, such as α_6-containing receptors, were based on the $\alpha_1\beta_2\gamma_2$ models. The resulting selection of $GABA_A$ receptor models that passed validation and for which uncertainty estimates have been made was subjected to putative active site analysis with PASS (Brady and Stouten, 2000), and the cavities that were identified by PASS were examined. The results were analyzed in the light of published experimental studies.

Results

Two generations of comparative models of the closed (tense) state of $GABA_A$ receptors are presented in this work. The older set, generated before 2BG9 (Unwin, 2005) was released, is based on three published sources (Brejc et al., 2001; Unwin et al., 2002; Miyazawa et al., 2003), and was built in several steps. First, the AChBP structure (Brejc et al., 2001) was used to model the β-folded domain of the nACh receptor's β, γ, and δ subunits. Then, the tense state described in (Unwin et al., 2002) was reconstructed for the nACh receptor α subunits. The individual subunits of this tense state model of the β-folded domain of the nACh receptor were then joined with the 1OED model (Miyazawa et al., 2003) of the helical domain to establish proper connectivity and "docked" at a distance just allowing van der Waals contacts. The resulting initial model of the combined domains of the nACh receptor was subjected to a standard simulated annealing protocol provided by the modeling program, without further refinement. This procedure was carried out repeatedly with different initial models to ensure that the domain junction converges to a consensus topology, which it did. Using this auxiliary nACh receptor model as template for the tense state, models of $GABA_A$ receptors (lacking the cytoplasmic domain) were then constructed.

After the release of 2BG9 (Unwin, 2005), this structure was used as single template to directly model $GABA_A$ receptors in the tense state, using the same alignments as with the "home-built" nACh receptor template, and the resulting models essentially replaced the first generation models. The two generations of models used in this study were analyzed in terms of similarities and differences. Within the limits of model uncertainty, the agreement was found to be very good. The older models, which were constructed by docking the extracellular domain (based on AChBP) and the helical domain (based on the nACh receptor helical domain fragment), displayed a small rigid-body shift in the relative orientation of the two domains compared with what is seen in 2BG9. This is often encountered when multiple templates are used (Marti-Renom et al., 2000). However, most results obtained with the first-generation models concerning interesting properties of the helical domain and the domain junction were confirmed by the second set of models. Thus, the results

presented below reflect findings that agree between both generations of models, except when stated otherwise.

Before the interpretation of computationally derived models, the expected degree of reliability needs to be assessed. In the following, putative structurally conserved elements of cys-loop receptors are identified and analyzed based on our

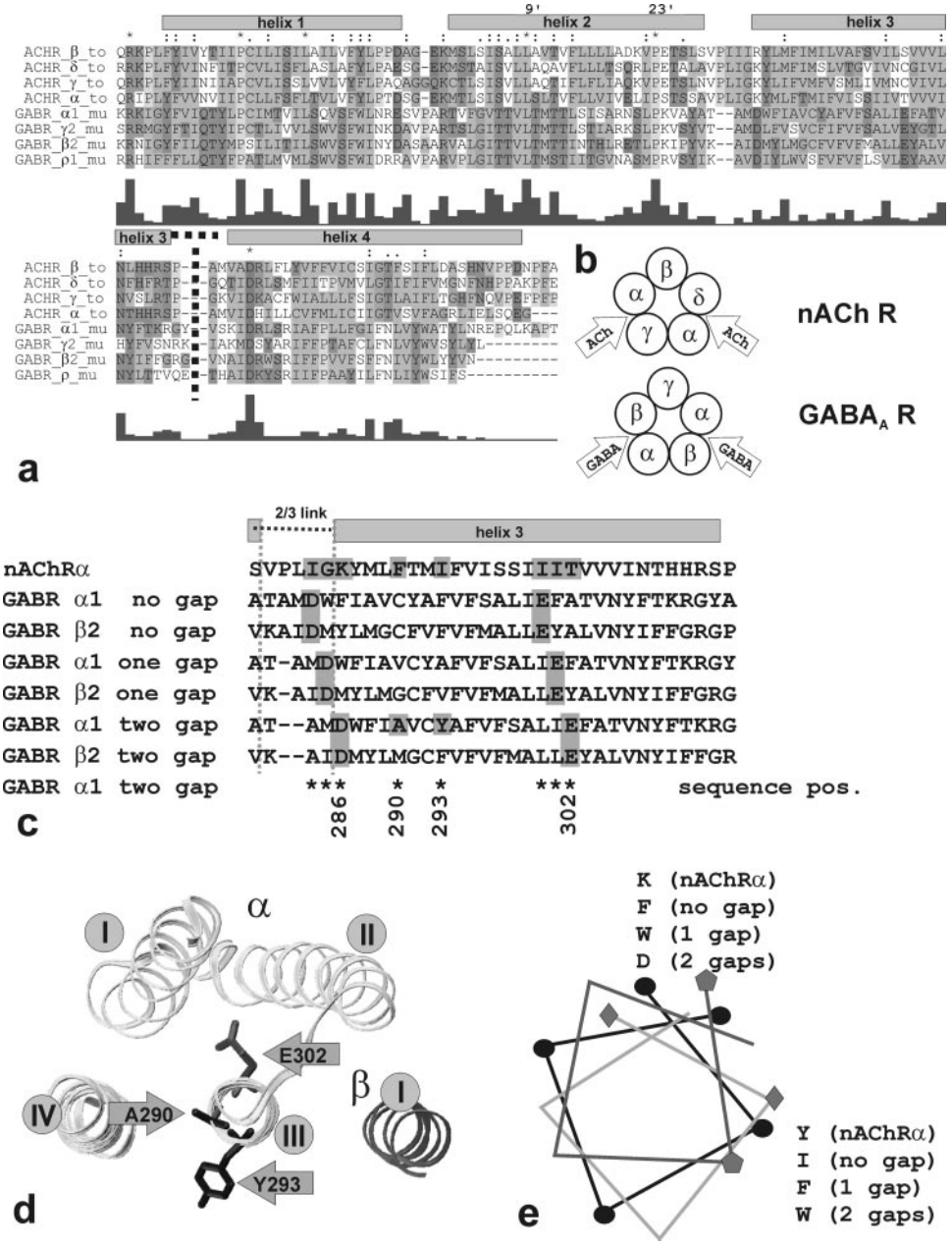

Fig. 1. Alignment of nACh and $GABA_A$ receptor helical domains. a, a subset of a superfamily alignment of the four segments that make up the helical (transmembrane) domain of the subunit chains is shown. The position of the missing "cytoplasmic loop" between helices 3 and 4 is indicated by a double-gap and a bold dotted line across all columns. Note that for helices 3 and 4, other alignment variants can be found, depending on the alignment parameters and on the number and choice of sequences that are included in a multisequence alignment. Standard Clustal (Thompson et al., 1997) symbols (*:.) are used to indicate degree of sequence conservation, also indicated by the bar graph beneath the alignment. b, subunit correspondence between nACh receptors and $GABA_A$ receptors is indicated by the schematic pentamers; arrows indicate agonist binding site locations. c, three different alignments for helix 3 of $GABA_A$ receptor α_1 and β_2 subunits with the corresponding nACh receptor α subunit segment from 1OED are shown. They result from placing zero, one, or two gaps in the alignment of the 2/3 linker between cation and anion channels. $GABA_A$ receptor residues α_1Asp286 and α_1Glu302, corresponding to a conserved Asp and Glu in anion channels, are highlighted to emphasize how they align with residues in the nAChR in the three alignment variants. The highly solvent accessible nACh receptor residues αPhe280 and αIle282, as well as $GABA_A$ receptor residues α_1Ala290 and α_1Tyr293, which can be cys-modified in appropriate mutants in the resting state, are also highlighted. d, model corresponding to the two-gap alignment of helix 3 of a $GABA_A$ receptor α subunit. Helix 3 is viewed from the N terminus and perpendicular to the paper plane, and all neighboring protein segments are also shown. Approximate side-chain orientations for the two cys-modifiable positions α_1Ala290C and α_1Tyr293C (wild-type side chains shown) are depicted, as well as the position for α_1Glu302 that is modifiable only under gating conditions. e, the helical wheel of the utmost N terminus of helix 3 is shown as schematic C-α trace; the black trace indicates the nACh receptor. The residue correspondence according to the three alignment variants shown in c is indicated for the first two helix positions. Natural variation in C-α position of distant homologs is indicated by two additional (gray) alternative helical wheels; the first two C-α atoms are indicated by different symbols. The indicated deviations correspond to C-α position changes in the order of 2 Å. Deviations of up to 5 Å are possible in structurally corresponding residue positions in homologs of low sequence identity.

models of nACh and $GABA_A$ receptors; then, the putative variable elements that lead to functional diversity are discussed for $GABA_A$ receptors. Figure 2 provides an overview of the topological features of the cys-loop receptor family.

Conserved Topological Properties of Cys-Loop Receptors. All subunits that form cys-loop receptors share a common architecture whose conserved elements are as follows: the "extracellular", β-rich domain consists of a variable N terminus (not shown) and two β sheets that form a "sandwich" (Brejc et al., 2001). They have been termed the "inner" and "outer" sheets (Unwin et al., 2002), indicating their luminal (inner) and abluminal (outer) localization, and are connected by the signature disulfide bridge.

The details of the architecture of the β-folded domain are shown in Fig. 2a. The inner sheet, indicated by light blue lines, connects the minus side diagonally with the plus side of the subunit on the luminal face and contains several key elements of agonist and drug action. So-called binding site "loops" D and E (minus side) and loop 2 (plus side) belong topologically to the inner sheet. Several of the linking segments that connect the inner sheet with the outer sheet also have been shown to be key players in the mediation of ligand effects; "loops" A and B (plus side), loop F (minus side), and loop 7 (the cys-loop), as well as the signature disulfide bridge (yellow double arrow in the figure), interconnect the two sheets.

The outer sheet, indicated by red connections, diagonally connects the plus side with the minus side of the subunit on the abluminal face, and provides loop C as functional segment. Strand 10 of the outer sheet terminates the β-folded domain and directly connects the plus side of the β-folded domain (loop C) with the minus side (pre-M1) of the helical pore domain. The topology diagram that shows how the peptide chain is organized into the two sheets is provided in Fig. 2b.

This particular topology, which couples the plus-side of the β-folded, agonist binding domain with the minus side of the helical domain and vice versa would imply transducing elements that make use of these cross-connections. Indeed, experimental results on the transducing elements of $GABA_A$ receptors (Kash et al., 2003, 2004a) strongly suggest such a "diagonal transduction"; GABA binding occurs at the β subunit's plus side. For consecutive gating to occur properly, the pre-M1 region of the β subunit (Kash et al., 2004a), which is localized at the minus side, was shown to be crucial. The α subunit, on the other hand, where GABA interacts with the minus side (loops D and E), seems to couple via the inner sheet and loop 2, which is localized at the plus side, as well as loop 7 (the "cys-loop") with the nearby M2/3 linker (Kash et al., 2003).

The helical pore-forming domain's architecture and topology is most likely conserved. In the published structures 1OED and 2BG9, four helical segments that pass the membrane form an "up-down" bundle that is interrupted by the cytoplasmic domain between helices 3 and 4. The positions of the four helices relative to the position within the pentameric complex are shown in Fig. 2c. Helix 1 is located in continuation of the minus side, helix 2 is pore-forming, helix 3 lies at the plus side, and helix 4 lies at the abluminal side of the subunit.

One of the striking features of the pore domain structure of the nACh receptor structural models 1OED and 2BG9 is the loose packing, which is likely to also be a conserved feature of this superfamily. This is not a general property of the four-helix bundle fold (Pearl et al., 2005), which contains a number of superfamilies (certain cytokines, for example), many of which are packed tightly. The loose packing is shown in Fig. 3, where all solvent-accessible space that is enclosed in a model of a $GABA_A$ receptor is filled with "pseudosolvent." If this buried pseudosolvent is quantified, the helical domain is

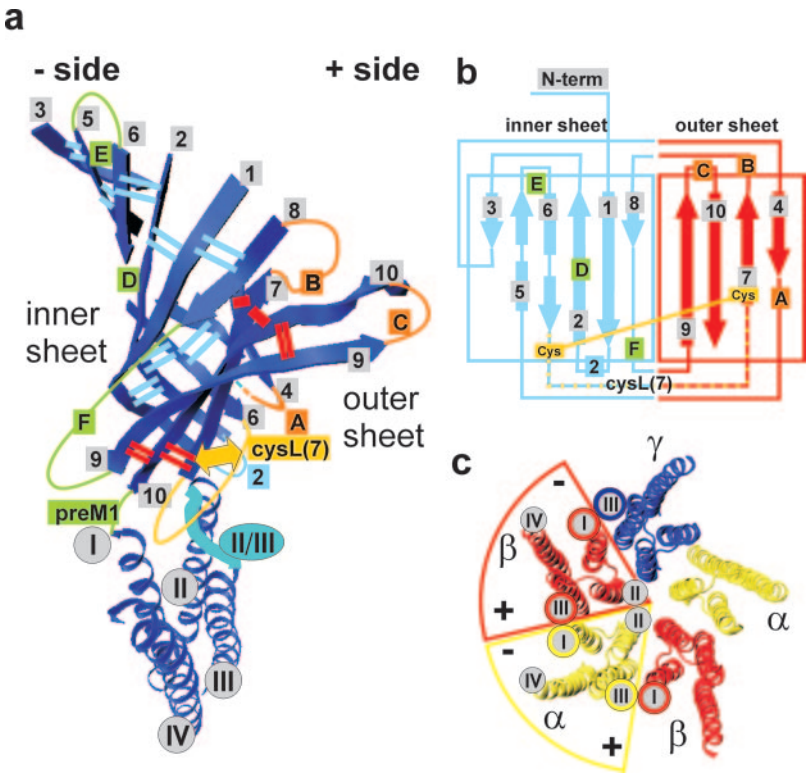

Fig. 2. Topology of cys-loop receptors. a, topology of a single subunit of a cys-loop receptor. The secondary structure motifs that are likely to be conserved are shown in ribbon representation, strand numbering is shown in Arabic numerals, and numbering of the membrane spanning helices is shown in Roman numerals. The important topologically conserved but structurally variable regions are indicated only schematically. The inner sheet's hydrogen bonds are schematically depicted in light blue and those of the outer sheet in red. All features that are associated with the plus side are shown in orange, and those that belong to the minus side are green. The cys-loop is yellow, and the disulfide bond is indicated as a yellow double arrow. b, the topology diagram of the β-folded domain is shown. The inner sheet-forming strands are light blue, and the outer sheet-forming strands are red. Note that strand length is not likely to be conserved in the superfamily and that short strands may not be conserved altogether. c, pentamer architecture of a $GABA_A$ receptor's helical domain, consisting of two α, two β, and one γ subunits. The view corresponds to a projection view to correctly show the localization of the four helices, curled around one another with respect to the subunit-interfaces. It can be seen that each interface is formed by helix 2 contacts, as well as by contacts of helix 1 of the minus side with helix 3 of the plus side subunit.

found to contain much more such putative pocket volume than the β-folded domain. The total enclosed pseudosolvent can be clustered into groups that represent different pockets, as indicated by different clusters of color in the figure. The possible roles of the cavities provided by the loosely packed helical domain will be discussed below.

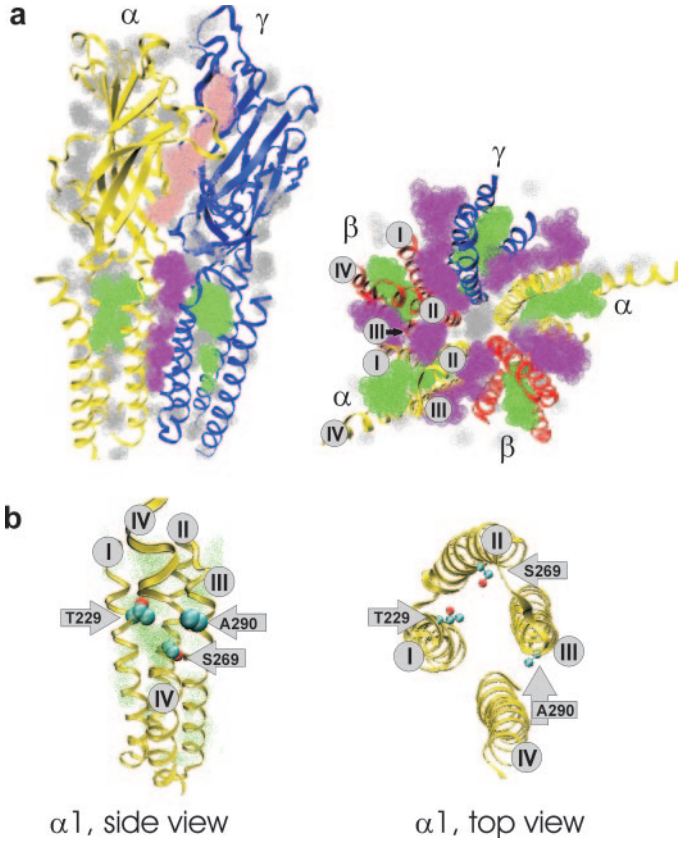

Fig. 3. Solvent-accessible space contained in $GABA_A$ receptor models. a, two views of a $GABA_A$ receptor model are shown to illustrate the solvent-accessible pockets, filled with "probe solvent". The left view shows a dimer from the outside of the pore. The right view is from outside the cell, with the β-folded domain invisible. The protein is shown in ribbon representation; the putative pockets identified with PASS (Brady and Stouten, 2000) are shown in dotted space-filling representation. Clusters of connected solvent accessible volumes that may correspond to drug binding pockets are highlighted by colors: pink is used for the space associated with the subunit-interface of the β-folded domain, purple for the large cavity present at the subunit interface at the junction between the β-folded and the helical domain that extends into the interface of the helical domains, and green for the cavity that is present inside each of the four-helix bundles of the subunit. Additional smaller clusters are shown in pale gray. It should be noted that because of the high uncertainty in side-chain positions, the total volume, shape, and electrostatic properties of the pockets varies considerably among models; in some models, some of the pockets may even be missing. Within the uncertainty of the method, it is also possible that there is significant communication between pink and purple as well as between green and purple pockets. For this illustration, a representative model was used whose properties correspond to what the majority of models display. b, helical domain of a $GABA_A$ receptor α_1 subunit shown from the side and from above. In the side view, helix 4 is broken to permit a view into the pocket enclosed by the four helices. The most likely positions of amino acid residues that mediate different ligand effects in $GABA_A$ receptor α_1 subunits are shown. According to our models, the intrasubunit green pocket seems to be lined, in α_1 subunits, by Thr229, which has been shown to account for lack of furosemide effect in α_1 and has a corresponding Ile in α_6. Residues α_1Ser269 in helix 2 and α_1Ala290 in helix 3 have been associated with the action of volatile anesthetics, and they are also part of the pocket. In glycine receptors, the residues homologous to Ser269 and Ala290 have been cross-linked in a double-Cys mutant. The residue positions shown in this figure are entirely consistent with this. The large apparent separation can easily be overcome by flexibility in helix 3 and might also be exaggerated by position errors caused by methodological limits discussed in the text.

The topology of the domain junction is likely to be highly conserved. Evidence for a well conserved topology at the domain junction was also provided by our modeling studies: In our first generation models of both nACh receptors and $GABA_A$ receptors that were based on two different and independently determined structures, the AChBP and the helical fragment of the nACh receptor, the extracellularly located loop 7 (cys-loop) and loop 2 interdigitate with the "M2/3" linker of the helical domain (Fig. 2a). This result was obtained by simply docking the two domains without using any extra restraints that would have forced a particular junction topology. The interlock of loops 2 and 7 with the M2/3 linker is in agreement with what has been suggested previously for the $GABA_A$ receptors, using combined experimental (Kash et al., 2003) and modeling (Kash et al., 2004c) approaches and was also confirmed by the latest release of the nACh receptor structure 2BG9 (Unwin, 2005). In fact, the agreement in the junction topology of our first generation models of the nACh receptor with the 2BG9 structural model was very good, and by far within the uncertainty that is intrinsic to the method.

Variable Elements of the Cys-Loop Receptor Architecture. Whereas architecture and topology of both the β-rich and the helical domains are conserved, the large functional diversity among cys-loop receptors must have corresponding structural equivalents, located mainly in the variable regions. The structural differences between the AChBP subunits and the β, γ, and δ subunits of the heteropentameric 2BG9 structure of the nACh receptor clearly demonstrate the variability of the β-stranded domain. The short strands, the loops, and the interface-forming segments of the individual subunits show significant structural diversity. This correlates well with results from our recent sequence conservation analysis (Ernst et al., 2003). The conservation indices presented there can still be used as a first guide for defining conserved and variable regions for estimating uncertainties in predictions. In addition, the strands of the topologically conserved sheets are organized in a unique way for each subunit, which is common for β-stranded fold families, but cannot be predicted in detail. The combined differences between AChBP and nACh receptor β, γ, and δ C-α coordinates are reflected in a root mean square deviation of 2.5 to 3 Å. Maximum differences of up to 12 Å between individual C-α atom pairs from sequence-aligned, highly variable regions are found. This is typically observed in β-stranded fold families, and it is to be expected that other superfamily members will display at least the same degree of variation.

The domain junction is known to display high variability within the conserved topology among different superfamily members (Kash et al., 2004b). Thus, in the conserved regions of the β-stranded domain and its junction with the helical domain (Ernst et al., 2003, and see below), model structures will be accurate up to the level of side-chain orientation. In the structurally variable regions, they will be correct at the level of topological position of segments. Armed with this knowledge, predictions can be interpreted and used properly.

In β-stranded folds, structural variation manifests in different patterns of sheet organization, whereas in helical folds, structural variability results in less obvious and more local changes, such as in different packing motifs. Thus, structural variability of this domain must be carefully ac-

counted for in modeling anion channels. Fig. 1a shows an alignment of the four helical segments of selected members of the superfamily. It is immediately obvious that there are very few absolutely conserved positions, and these are predominantly in helices 1 and 2, as indicated by asterisks in Fig. 1a. In helices 3 and 4, conservation among cation channels, as well as among anion channels, is high, but low between cation and anion channels. The questions associated with identifying the homology model that "best" predicts $GABA_A$ receptor structure will be addressed in more detail below.

Conservation in Helices 1 and 2. Helix 1 is characterized by a conserved Pro residue, which presumably is structurally equivalent in all family members. A second position in helix 1 is highly conserved, namely the Leu marked in the alignment in Fig. 1a by an asterisk. This position is hydrophobic in all superfamily members; most have a Leu in this position. The conserved Pro, together with proper alignment of hydrophobic and nonhydrophobic positions in all members of the superfamily, implies that helix 1 is closely conserved in the structural sense. This means that the orientation of sidechains with respect to the surroundings of helix 1 will be similar to 1OED and 2BG9 in the other receptors.

In helix 2, the presence of two conserved residues (Leu and Pro at index positions 9′ and 23′, respectively, Fig. 1a) strongly implies conserved structure. Indeed, in our models based on 1OED and 2BG9, the same side-chains that have been mapped as pore-lining by experimental approaches (Xu and Akabas, 1996) are found along the central pore, thus confirming close conservation.

Thus, close structural similarity can be assumed in helices 1 and 2 for all members of the superfamily.

Lack of Conservation in Helices 3 and 4. In aligning helix 3 between cation and anion channels, two problems arise: there are no absolutely conserved residues, and the contents of hydrophobic amino acids is high. This leads to significant ambiguities in the alignment. Therefore, multiple alignment variants, as well as multiple degrees of "homology" (or "conservedness") have to be considered in computing and interpreting models. In homologs that share sequence identity below 30%, as is the case here, insertions/deletions (so-called "indels") are commonly found in linkers connecting secondary structure elements and must be considered in constructing alignments for modeling purposes.

In Fig. 1c, three variants of aligning helix 3 between cation channels and anion channels are shown. They are generated by placing zero, one, or two gaps into the 2/3 linker, and they all obtain roughly equal alignment scores because of the hydrophobic character of the aligned segments. Thus, alignment scores do not help in selecting among these variants, but gap penalties become high if more than two gaps are introduced. A clear ranking also could not be established by computing and scoring the corresponding models.

Because it is not feasible to identify the most convincing helix 3 alignment by purely computational means, we have used a combined approach of relating local model properties to experimental data to discriminate between the possible variants. Extensive substituted cysteine accessibility mapping data (Akabas, 2004) on the accessibility of helix 3 residues of $GABA_A$ receptor α1 subunits, in the resting state and under the influence of various ligands, are available (Williams and Akabas, 2002; Akabas, 2004; Jung et al., 2005) (Fig. 4). The following observations from the substituted cysteine accessibility mapping studies are informative for the alignment problem.

In the resting state, only α_1A290C and α_1Y293C, shaded in light blue in Fig. 4 (gray in Fig. 1), could be modified with Cys-modifying reagents. This yields the labeling pattern AxxY, where x denotes a presumably inaccessible position. This pattern was then compared with side-chain accessibility in the nACh receptor structures 1OED and 2BG9, as determined with the procheck program (Laskowski et al., 1993). Near the N terminus of helix 3 of the nACh receptor, there are also two significantly more solvent accessible residues, αPhe280 and αIle282, yielding the pattern FxxI (shaded gray in Fig. 1c). Thus, it is reasonable to align the AxxY motif in the $GABA_A$ receptor α_1 with the FxxI motif in the nACh receptor. This alignment corresponds to the variant with two gaps in the linker.

Further support for this two-gap hypothesis comes from three additional observations: first, in this alignment variant, an aspartate (α_1Asp286) that is conserved at the N terminus of helix 3 in anion channels ends up aligned with a conserved basic position in the cation channels, as seen in Fig. 1c. This makes more sense than what is seen in the other two alignment variants. Second, and even more convincing, α_1Ala290 and homologous residues near the N terminus of helix 3 have been found to be part of a hypothetical binding pocket for anesthetics (Jenkins et al., 2001), and the two-gap alignment places these residues indeed in a pocket-lining position, as discussed in detail below. Third, the position α_1E302C was found to be accessible for Cys-modifying reagents only in the presence of gating concentrations of GABA or propofol (Williams and Akabas, 2002) (Fig. 4) and thus is thought to be buried in the resting state. Only the two-gap alignment models position this residue in a buried position in which the acidic side chain does not interfere with hydrophobic packing. The approximate position of this side chain, as well as the two residues α_1Ala290 and α_1Tyr293, as seen in the 2-gap models, is shown in Fig. 1d. From all this, we conclude that the 2-gap alignment generates model structures that resemble the true structure better than other alignment variants. This conclusion is supported by even more experimental evidence, as discussed below.

Helix 4 is also characterized by very low sequence similarity between cation and anion channels, apart from the high degree of hydrophobic amino acids in the membrane-spanning portion. An aspartate residue, which occurs in all superfamily members, suggests a conserved function for this position, which in turn suggests structural homology. Thus, the most plausible alignment variant for this segment is the one shown in Fig. 1a, which also yields models with reasonable scores.

Nevertheless, despite the fact that the two-gap model of helix 3 and the conserved aspartate hypothesis for helix 4 seem highly plausible, high uncertainty is associated with coordinates of amino acid residues in these segments of the comparative models because of the low homology between cation and anion channels in the helical domain, with sequence identity ranging only from 13 to 21%. At such low sequence similarity, side-chain interactions and packing properties are generally not conserved. From structure comparison methods (Prlic et al., 2000), it is known that structurally equivalent amino acids in pairs of related and super-

posed structures can have Cα and Cβ distances from each other of up to 5 Å. This natural variation is shown schematically in Fig. 1e for the Cα positions of helix 3 in the nACh receptor α subunit. $GABA_A$ receptor residues corresponding to the nACh receptor residues αLys276 and αTyr277 are shown according to zero-, one-, or two-gap alignment. This shows the changes in amino acid side-chain positions resulting from different alignments. The additional variation that comes from low homology is sketched by the gray helices in Fig. 1e (different symbols are used to represent alternative C-α positions), indicating how far away from the αLys276 position these residues could be located and still be well within the definition of "structurally equivalent" (Prlic et al., 2000). This results from the fact that the natural variation shown in Fig. 1e can be neither predicted nor modeled. In general, comparative models have a tendency to resemble their "parent structures" too closely, and energy minimization or simulation runs will not result in more "true" structures (Schonbrun et al., 2002). Approaches that are more sophisticated are cost-prohibitive for models of this size and are still in the stage of development. The "true" structure thus can only be determined by experimental means. Despite these caveats, models still can be used to derive valuable predictions. At low sequence similarity, multiple models based on distinct input, such as different alignments, loop conformations, and templates (if available), must generally be used. In the conserved regions, these models will yield consensus predictions. In the variable regions, the different predictions that "survive" standard validation must be analyzed on a statistical basis. Thereafter, suitable experimental data could be used as spatial restraints in building improved model structures.

Pockets in and around the Helical Domain in the Closed, Tense State. Putative binding sites can be identified in structural models using PASS (Brady and Stouten, 2000) or similar tools. Even in models of moderate accuracy, the overall pocket organization can be determined with such an approach. The pockets contained in the extracellular domain at the intersubunit interfaces have been discussed previously (Ernst et al., 2003). In this work, we focus on the pockets that are formed, fully or partly, by segments from the helical domain. As can be seen in Fig. 3, two "types" of cavities are found by pocket-finding algorithms: a rather large cavity is present inside of each of the four helix bundles, shown in green in Fig. 3. In addition, and as has been noted before (Miyazawa et al., 2003), another large cavity exists between the subunits at and below the domain junction, shown in purple in Fig. 3.

Although the shape and volume of the pockets varies with different model variants, the cavities as such are present in the overwhelming majority of models, and the identity of the segments that form the cavities is not affected by ambiguities in helices 3 and 4. However, predictions of the cavity-forming segments now can be refined by subsequent experimental mapping, which in turn will lead to models with a more defined pocket geometry.

It is interesting that in some models, the intersubunit (purple) pockets of the helical domain seem to communicate

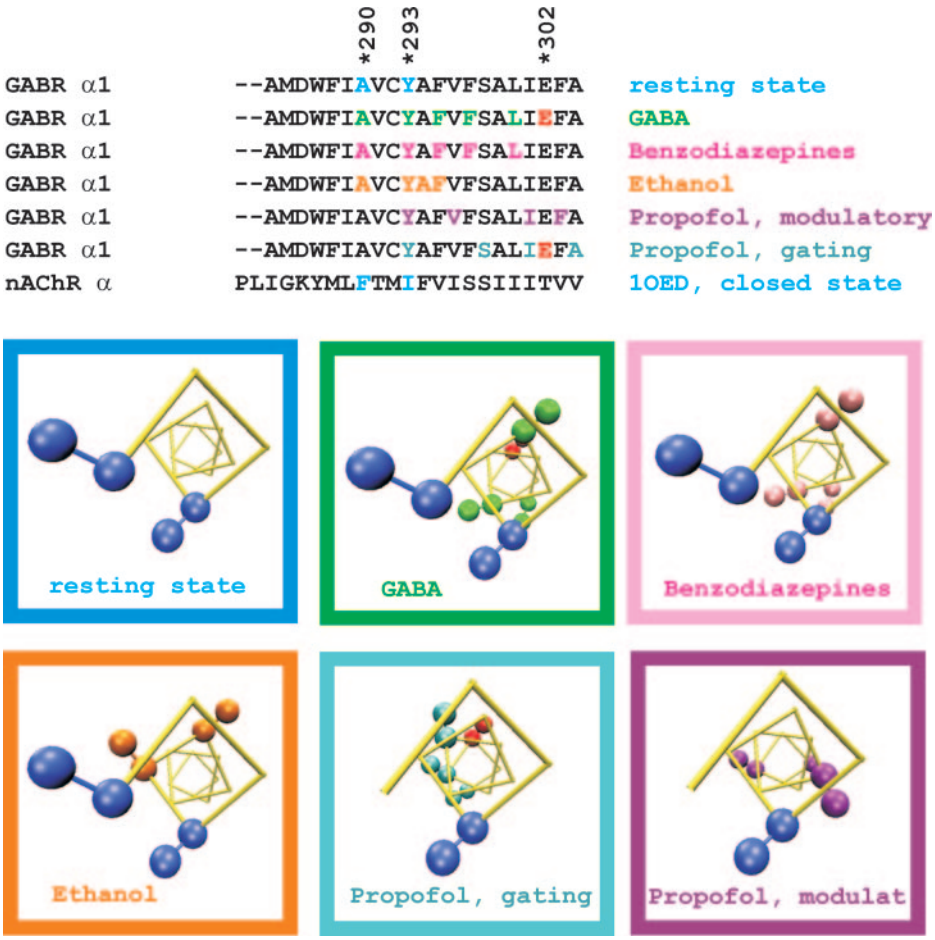

Fig. 4. Drug-induced changes in the accessibility of amino acid residues in helix 3. The sequence of the $GABA_AR$'s α1 helix 3 segment is shown; cysteine-modifiable positions are color-coded. The helix 3 sequence of the torpedo nACh receptor α subunit is shown in the bottom line, in the alignment variant featuring two gaps in the 2/3 linker. Each experimental condition is characterized by a unique set of modifiable positions in helix 3, indicating great conformational flexibility of this segment. In general, presence of agonistic or positively modulating agents increases accessibility of helix 3. The corresponding sidechains' Cα and Cβ positions are shown in a model of helix 3, viewed from N terminus and pointing straight through the plane of the paper.

with their extracellular counterparts. Thus, the interface between subunits might contain a continuous groove that might have more than one function.

The intrasubunit ("green") pockets that are confined by the four helices of each subunit contain a number of amino acid residues well investigated by various experimental means. In α subunits, residues in helices 1, 2, and 3 have been shown to be key components in binding or action of different modulatory drugs: α_6Ile228 of helix 1 (corresponding to α_1Thr229) determines α selectivity of furosemide (Thompson et al., 1999) and is part of the wall of the "green" pocket in α subunits. See Fig. 3b for a view of this pocket from two directions. α_1Ser269 of helix 2 has been proposed to be part of a pocket for volatile anesthetics (Jenkins et al., 2001); this residue also lines this pocket. α_1Ala290 (rat sequence numbering; human is α_1Ala291) of helix 3 has also been proposed to be part of the "anesthetics pocket" (Jenkins et al., 2001) and is also found in the pocket wall in models derived from the alignment variant bearing two gaps. (see Fig. 3b)

In β subunits, residues in helices 2 and 3, in positions homologous to those discussed above, have also been shown to be key components in binding or action of modulatory drugs. Residue β_1Ser265 corresponds to residue α_1Ser269 in α subunits. β_2 and β_3 have an Asn at the homologous position. This Ser/Asn polymorphism is critical for the additional β subunit selectivity of furosemide action (Thompson et al., 1999). The same Ser/Asn polymorphism of the β subunits also accounts for the β subtype selectivity of loreclezole, etomidate, and other related substances (Belelli et al., 2003). Thus, the Ser/Asn position at β_1Ser265 (corresponding to α_1Ser269) is part of the "green" pocket and may be part of a binding site for these substances.

Finally, the position for the side chains of the preM1 point mutants β_2G219X could not be localized with any reliability in the old generation of models. But in the 2BG9-derived models, these side chains seem to be either part of the "green" pocket or to control the access pathway to the pocket. This could nicely explain that substitution of β_2Gly219 with larger residues leads to a reduced barbiturate sensitivity of the receptor and that the reduction increases with increasing size of the substituent (Carlson et al., 2000).

Discussion

Models of the β-Folded and Helical Domains of $GABA_A$ Receptors Agree with Experimental Data. In the present study, we have modeled the β-folded "extracellular" and the helical "transmembrane" domain of electric organ nACh receptors in the closed, "tense" state on the basis of available structural data before the release of the 2BG9 coordinates. Using this model as a template, we then proceeded to model the combined β-folded and helical domains of $GABA_A$ receptor subtypes. Additional models based on 2BG9 were added after these coordinates became available. Thereafter, all $GABA_A$ receptor models were evaluated for model uncertainty and validated by comparison with known data. In agreement with experimental evidence, we find that the junction between the β-folded and helical domains is formed by loops 2 and 7 of the extracellular domain spontaneously interdigitating with the 2/3 linker of the helical domain (Fig. 2a). This junction topology is likely to be conserved, as indicated by the observation that only loops 2, 7 (cys-loop), and 9 (F-loop) (see Fig. 2a) had to be modified in the AChBP portion of chimeras consisting of an N-terminal AChBP and the helical domain of the $5HT_3$-receptor to engineer receptor-like properties (Bouzat et al., 2004). Nevertheless, different superfamily members and even different subunits of a single receptor class, for example the α and β subunits of $GABA_A$ receptors (Kash et al., 2003, 2004a), employ slightly different mechanisms in transducing conformational changes.

Although the overall architecture and topology of the helical domain is conserved within the superfamily, alignment of the four helical segments of cys-loop receptors indicate that only helices 1 and 2 are closely conserved in a structural sense, allowing a more or less correct prediction of amino acid side chain positions. In helices 3 and 4, there are quite some ambiguities in the alignment. We find the best overall performance for our $GABA_A$ receptor models when two gaps in the alignment are introduced in the M2/3 linker. Under these conditions, two amino acid residues ($GABA_A$ receptor α_1Ala290 and α_1Tyr293 within the resulting helix 3 that are solvent-accessible in the resting state of $GABA_A$ receptors as indicated by experimental data) are located in positions homologous to those of solvent-accessible residues of the nACh receptor.

The Existence of Inter- and Intrahelical Pockets Suggests Multiple Drug Binding Sites. In contrast to a previous model of $GABA_A$ receptors, in which the β-folded domain was combined with a transmembrane domain based on the structures of nonrelated proteins and was described as "tightly packed" (Trudell and Bertaccini, 2004), the helical domain of models based on the nACh receptor structures is loosely packed (Miyazawa et al., 2003). Therefore, they feature a fairly large content of "putative pocket volume" (Fig. 3). The pockets can be grouped into two main clusters. One of these is located at the subunit interfaces. In some models, they form a continuum from the extracellular domain to deep into the helical domain. They have been proposed to be needed by the movement of helix 2 in gating of the ion channel (Unwin, 2003). Because the extracellular pockets between subunits contain the GABA and the benzodiazepine binding sites of $GABA_A$ receptors, it is quite conceivable that their extension into the junctional and helical domains can also be used by drugs to modulate the function of receptors.

Additional cavities are present inside of each of the four-helix bundles of the subunits (green pockets in Fig. 3). Assuming the two-gap alignment variant for helix 3, amino acid residues in helices 1 (α_1Thr229/α_6Ile228), 2 (α_1Ser269/β_1Ser265/$\beta_{2/3}$Asn265) and 3 (α_1Ala290/β_2Met286) of α or β subunits, previously demonstrated to be important for the actions of volatile and intravenous anesthetics, furosemide, etomidate, and barbiturates, are found in our models to line the wall of the respective intrahelical pockets.

Independent evidence for this conclusion comes from experiments on glycine receptors. Cysteines replacing the glycine receptor residues homologous to α_1Ser269 (β_1Ser265) and α_1Ala290 (β_2Met286) can form a disulfide bond (Lobo et al., 2004). Because residue α_1Ser269 is oriented toward the center of the four-helix bundle, as indicated by experimental evidence (Mascia et al., 2000) and by the conserved side chain positions of helix 2 (see 1OED and 2BG9), disulfide formation is possible only if the glycine receptor residue homologous to α_1Ala290 (β_2Met286) is also accessible from the pocket inside the helical domain. Considering the uncertainty of model

coordinates and the apparently significant flexibility of helix 3 (Akabas, 2004), a disulfide bridge crossing the intrasubunit pocket can easily be envisioned in models based on the two-gap alignment.

In $GABA_A$ receptor α subunits, residues α_1Ser269 and α_1Ala290 have been proposed previously to be part of a binding pocket for volatile anesthetics (Mascia et al., 2000). Strong support for a role of this intrasubunit pocket as a possible drug binding site comes from the fact that in β subunits, helix 3 mutant β_2M286C (homolog of α_1Ala290) has been shown to be protected by propofol in a dose-dependent manner against covalent modification by cys-reactive reagents (Bali and Akabas, 2004).

The cumulative evidence for the existence of this pocket type as a conserved feature of $GABA_A$ and glycine receptor subunits is thus impressive. Because functional modulation of $GABA_A$ receptors by furosemide or certain anesthetics can be influenced by amino acid residues in α as well as β subunits, it is tempting to speculate that multiple binding sites for these compounds are present in the intrasubunit ("green") pockets of different $GABA_A$ receptor subunits. Depending on the specific electrostatic and steric interactions of drugs with these pockets, they could stabilize different conformations of the receptors, giving rise to their GABA-modulating, direct gating, or inhibitory action at different drug concentrations. The entire helical domain, however, seems also to be crucial for transduction of ligand binding to gating or allosteric modulation. This is indicated by the effects of point mutants in this region on GABA action and benzodiazepine modulation (Boileau and Czajkowski, 1999) and by conformational changes in the helical domain induced by drug binding (see below).

Structural Models Provide Clues on Conformational Changes Induced by Ligand Binding. Helix 3 of $GABA_A$ receptor α_1 subunits has been point-mutated in 15 positions and probed with cysteine modifying reagents under the influence of various modulatory and GABA-mimetic drugs (Williams and Akabas, 2002; Akabas, 2004; Jung et al., 2005). Data indicate that the solvent accessibility of helix 3 residues changes differentially with different drugs (Fig. 4) pointing toward large conformational flexibility of helix 3. The resting state displays detectable Cys-modifying reactivity only in two positions near the N terminus, α_1Ala290 and α_1Tyr293; the portion of the helix closer to the C-terminus seems to be fairly well buried under this condition. GABA, benzodiazepines, ethanol, and propofol increase the total number of modifiable positions. The individual SCAM "fingerprints" (Fig. 4) imply that each substance induces a distinct functional state. It is interesting that position α_1E302C was found modifiable only in the presence of gating concentrations of GABA or propofol. Thus, either the segment of helix 3 in which α_1Glu302 is located, or its neighborhood, namely helix 2, must undergo major rearrangement upon gating for E302C to become modifiable. Helix 2 forms the ion gate; thus, in agreement with previous proposals (Unwin, 2003; Goren et al., 2004), it is plausible to assume that helix 2 moves.

Benzodiazepine modulation induces a conformation very closely resembling the GABA-induced gating conformation, lacking only E302C in its fingerprint. This supports the conclusion that benzodiazepine binding causes a conformational change that is directly transduced into the helical domain. In contrast, the states induced by two different concentrations of propofol are quite distinct from each other, supporting the notion that propofol interacts with an additional binding site at gating concentrations. In addition, gating concentrations of propofol seem to induce a conformation in α subunits that is completely different from the gating conformation induced by GABA, consistent with a completely different mechanism of action of these compounds.

Further mapping of drug-induced changes in solvent accessibility of all four helices as well as of other parts of the receptors using our models as a guide will delineate similarities and differences in drug action and drug-induced conformational changes. Model structures can then be used to visualize these changes and to describe the dynamics of these important receptors.

In summary, by using available information on the structure of the AChBP and the nACh receptor, we were able to develop models of the $GABA_A$ receptor that not only are consistent with most experimental data but also could explain experimental observations and propose the location of putative drug binding sites. These models can now be used to design new experiments for clarification of pharmacological and structural questions as well as to shed light on conformational changes during binding of agonists, gating, and allosteric modulation of these receptors. Overall, these experiments will lead to an improvement in the accuracy of the models and finally pave the way for a structure-based drug design. Structure files are available in the Supplemental data.

References

Akabas MH (2004) GABAA receptor structure-function studies: a reexamination in light of new acetylcholine receptor structures. *Int Rev Neurobiol* **62:**1–43.

Bali M and Akabas MH (2004) Defining the propofol binding site location on the $GABA_A$ receptor. *Mol Pharmacol* **65:**68–76.

Belelli D, Muntoni AL, Merrywest SD, Gentet LJ, Casula A, Callachan H, Madau P, Gemmell DK, Hamilton NM, Lambert JJ, et al. (2003) The in vitro and in vivo enantioselectivity of etomidate implicates the GABAA receptor in general anaesthesia. *Neuropharmacology* **45:**57–71.

Bertaccini E and Trudell JR (2001) Molecular modeling of ligand-gated ion channels: progress and challenges. *Int Rev Neurobiol* **48:**141–166.

Boileau AJ and Czajkowski C (1999) Identification of transduction elements for benzodiazepine modulation of the GABA(A) receptor: three residues are required for allosteric coupling. *J Neurosci* **19:**10213–10220.

Bouzat C, Gumilar F, Spitzmaul G, Wang HL, Rayes D, Hansen SB, Taylor P, and Sine SM (2004) Coupling of agonist binding to channel gating in an ACh-binding protein linked to an ion channel. *Nature (Lond)* **430:**896–900.

Brady GP and Stouten PFW (2000) Fast prediction and visualization of protein binding pockets with PASS. *J Comput-Aided Mol Des* **14:**383–401.

Brejc K, van Dijk WJ, Klaassen RV, Schuurmans M, van Der Oost J, Smit AB, and Sixma TK (2001) Crystal structure of an ACh-binding protein reveals the ligand-binding domain of nicotinic receptors. *Nature (Lond)* **411:**269–276.

Carlson BX, Engblom AC, Kristiansen U, Schousboe A, and Olsen RW (2000) A single glycine residue at the entrance to the first membrane-spanning domain of the γ-aminobutyric acid type A receptor β_2 subunit affects allosteric sensitivity to GABA and anesthetics. *Mol Pharmacol* **57:**474–484

Ernst M, Brauchart D, Boresch S, and Sieghart W (2003) Comparative modeling of GABA(A) receptors: limits, insights, future developments. *Neuroscience* **119:**933–943.

Goren EN, Reeves DC, and Akabas MH (2004) Loose protein packing around the extracellular half of the $GABA_A$ receptor β1 subunit M2 channel-lining segment. *J Biol Chem* **279:**11198–11205.

Hinsen K (2000) The molecular modeling toolkit: a new approach to molecular simulations. *J Comp Chem* **21:**79–85.

Jenkins A, Greenblatt EP, Faulkner HJ, Bertaccini E, Light A, Lin A, Andreasen A, Viner A, Trudell JR, and Harrison NL (2001) Evidence for a common binding cavity for three general anesthetics within the GABAA receptor. *J Neurosci* **21:** RC136.

Jung S, Akabas MH, and Harris RA (2005) Functional and structural analysis of the $GABA_A$ receptor α_1 subunit during channel gating and alcohol modulation. *J Biol Chem* **280:**308–316.

Kash TL, Dizon MJ, Trudell JR, and Harrison NL (2004a) Charged residues in the β_2 subunit involved in $GABA_A$ receptor activation. *J Biol Chem* **279:**4887–4893.

Kash TL, Jenkins A, Kelley JC, Trudell JR, and Harrison NL (2003) Coupling of agonist binding to channel gating in the GABA(A) receptor. *Nature (Lond)* **421:** 272–275.

Kash TL, Kim T, Trudell JR, and Harrison NL (2004b) Evaluation of a proposed

mechanism of ligand-gated ion channel activation in the GABAA and glycine receptors. *Neurosci Lett* **371:**230–234.
Kash TL, Trudell JR, and Harrison NL (2004c) Structural elements involved in activation of the gamma-aminobutyric acid type A (GABAA) receptor. *Biochem Soc Trans* **32:**540–546.
Laskowski RA, MacArthur MW, Moss DS, and Thornton JM (1993) PROCHECK: a program to check the sterochemical quality of protein structures. *J Appl Cryst* **26:**283–291.
Lobo IA, Trudell JR, and Harris RA (2004) Cross-linking of glycine receptor transmembrane segments two and three alters coupling of ligand binding with channel opening. *J Neurochem* **90:**962–969.
Marti-Renom MA, Stuart AC, Fiser A, Sanchez R, Melo F, and Sali A (2000) Comparative protein structure modeling of genes and genomes. *Annu Rev Biophys Biomol Struct* **29:**291–325.
Mascia MP, Trudell JR, and Harris RA (2000) Specific binding sites for alcohols and anesthetics on ligand-gated ion channels. *Proc Natl Acad Sci USA* **97:**9305–9310.
Miyazawa A, Fujiyoshi Y, and Unwin N (2003) Structure and gating mechanism of the acetylcholine receptor pore. *Nature (Lond)* **423:**949–955.
Pearl F, Todd A, Sillitoe I, Dibley M, Redfern O, Lewis T, Bennett C, Marsden R, Grant A, Lee D, et al. (2005) The CATH Domain Structure Database and related resources Gene3D and DHS provide comprehensive domain family information for genome analysis. *Nucleic Acids Res* **33:**D247–D251.
Peters JA, Kelley SP, Dunlop JI, Kirkness EF, Hales TG, and Lambert JJ (2004) The 5-hydroxytryptamine type 3 (5-HT_3) receptor reveals a novel determinant of single-channel conductance. *Biochem Soc Trans* **32:**547–552.
Prlic A, Domingues FS, and Sippl MJ (2000) Structure-derived substitution matrices for alignment of distantly related sequences. *Protein Eng* **13:**545–550.
Sali A and Blundell TL (1993) Comparative protein modelling by satisfaction of spatial restraints. *J Mol Biol* **234:**779–815.
Schonbrun J, Wedemeyer WJ, and Baker D (2002) Protein structure prediction in 2002. *Curr Opin Struct Biol* **12:**348–354.
Shi J, Blundell TL, and Mizuguchi K (2001) FUGUE: sequence-structure homology recognition using environment- specific substitution tables and structure-dependent gap penalties. *J Mol Biol* **310:**243–257.
Sieghart W (1995) Structure and pharmacology of γ-aminobutyric $acid_A$ receptor subtypes. *Pharmacol Rev* **47:**181–234.
Sieghart W and Sperk G (2002) Subunit composition, distribution and function of GABA(A) receptor subtypes. *Curr Top Med Chem* **2:**795–816.
Thompson JD, Gibson TJ, Plewniak F, Jeanmougin F, and Higgins DG (1997) The CLUSTAL_X windows interface: flexible strategies for multiple sequence alignment aided by quality analysis tools. *Nucleic Acids Res* **25:**4876–4882.
Thompson JD, Higgins DG, and Gibson TJ (1994) CLUSTAL W: improving the sensitivity of progressive multiple sequence alignment through sequence weighting, position-specific gap penalties and weight matrix choice. *Nucleic Acids Res* **22:**4673–4680.
Thompson SA, Arden SA, Marshall G, Wingrove PB, Whiting PJ, and Wafford KA (1999) Residues in transmembrane domains I and II determine γ-aminobutyric acid type A receptor subtype-selective antagonism by furosemide. *Mol Pharmacol* **55:**993–999.
Trudell JR and Bertaccini E (2004) Comparative modeling of a GABAA alpha1 receptor using three crystal structures as templates. *J Mol Graph Model* **23:**39–49.
Unwin N (2003) Structure and action of the nicotinic acetylcholine receptor explored by electron microscopy. *FEBS Lett* **555:**91–95.
Unwin N (2005) Refined structure of the nicotinic acetylcholine receptor at 4A resolution. *J Mol Biol* **346:**967–989.
Unwin N, Miyazawa A, Li J, and Fujiyoshi Y (2002) Activation of the nicotinic acetylcholine receptor involves a switch in conformation of the alpha subunits. *J Mol Biol* **319:**1165–1176.
Williams DB and Akabas MH (2002) Structural evidence that propofol stabilizes different GABA(A) receptor states at potentiating and activating concentrations. *J Neurosci* **22:**7417–7424.
Xu M and Akabas MH (1996) Identification of channel-lining residues in the M2 membrane-spanning segment of the GABA(A) receptor alpha1 subunit. *J Gen Physiol* **107:**195–205.

Address correspondence to: Univ. Prof. Dr. Werner Sieghart, Center for Brain Research, Medical University Vienna, Division of Biochemistry and Molecular Biology, Spitalgasse 4, A-1090 Vienna, Austria. E-mail: werner.sieghart@meduniwien.ac.at